Observation of $\psi(3686) \to \bar{\Lambda}\Lambda\eta'$ decay

BESIII Collaboration; Ablikim, M.; Achasov, M.N.; Adlarson, P.; Ai, X.C.; Aliberti, R.; Amoroso, A.; Kalantar-Nayestanaki, Nasser; Kavatsyuk, Myroslav; Messchendorp, Johan

Published in:
Physical Review D

DOI:
10.1103/PhysRevD.108.112014

Observation of $\psi(3686) \to \Lambda\bar{\Lambda}\eta'$ decay

M. Ablikim *et al.*[*]
(BESIII Collaboration)

(Received 21 September 2023; accepted 22 November 2023; published 27 December 2023)

Using a sample of $(27.12 \pm 0.14) \times 10^8$ $\psi(3686)$ events collected with the BESIII detector, the decay $\psi(3686) \to \Lambda\bar{\Lambda}\eta'$ with η' subsequently decaying into $\gamma\pi^+\pi^-$ and $\eta\pi^+\pi^-$ is observed for the first time. The branching fraction of $\psi(3686) \to \Lambda\bar{\Lambda}\eta'$ is measured to be $(7.34 \pm 0.94(\text{stat}) \pm 0.43(\text{sys})) \times 10^{-6}$. No resonant structures are evident in the $\Lambda\eta'$, $\bar{\Lambda}\eta'$ and $\Lambda\bar{\Lambda}$ mass spectra.

DOI: 10.1103/PhysRevD.108.112014

I. INTRODUCTION

Quantum chromodynamics (QCD), the theory describing the strong interaction, has been tested thoroughly at high energy. However, in the medium-energy region, theoretical calculations based on first principles are still unreliable since the nonperturbative contribution is significant and models must be employed. Charmonium resonances, as bound states of a charm and an anticharm quark, are governed by long-range interactions and exist on the boundary between the perturbative and nonperturbative regimes in QCD [1,2]. Therefore, the study of charmonium decays [3,4] can provide valuable inputs for gaining a better understanding of the structure of these states and for improving our knowledge of QCD. The BESIII experiment has collected large data samples of J/ψ and $\psi(3686)$ events, making possible the study of decay channels of these states, many with complicated intermediate structures.

The decays of J/ψ and $\psi(3686)$ mesons into baryon pairs have been understood in terms of $c\bar{c}$ annihilations into three gluons or a virtual photon [5]. However, three-body decays, for example $J/\psi(\psi(3686)) \to \Lambda\bar{\Lambda}P$, where "$P$" represents a pseudoscalar meson such as π^0, η, or η', warrant further study because of the potentially important contribution of intermediate states. An excited Λ state, $\Lambda(1670)$, was observed in the $\Lambda\eta$ mass spectra in the near-threshold reaction $K^- p \to \Lambda\eta$ [6]. It is generally accepted today as the SU(3) octet partner of $\Lambda(1800)$ [7]. The $\Lambda(1670)$ is of special interest because it is one of the two baryon resonances known to have appreciable decays involving the η meson except for $\Lambda(1600)$. Recently the $\Lambda(1670)$ has been found to make a significant contribution to the decay $\psi(3686) \to \Lambda\bar{\Lambda}\eta$ [8,9]. However, the decay of $J/\psi \to \Lambda\bar{\Lambda}\eta'$ is hard to observe experimentally because of the limited phase space, while the study of $\psi(3686) \to \Lambda\bar{\Lambda}\eta'$ is feasible but has not been attempted yet.

Since the excitation spectra of most hyperons are still not well understood [10,11], it is important to search for excited hyperons which have not yet been observed. The decay $\psi(3686) \to \Lambda\bar{\Lambda}\eta'$ provides an opportunity to search for potential Λ excitations. A sample of $(27.12 \pm 0.14) \times 10^8$ $\psi(3686)$ events [12] produced in e^+e^- annihilations [7] has been collected with the BESIII detector, which allows for the experimental study of the decay $\psi(3686) \to \Lambda\bar{\Lambda}\eta'$.

II. DETECTOR AND MONTE CARLO SIMULATION

The BESIII detector [13] records symmetric e^+e^- collisions provided by the BEPCII storage ring [14] in the center-of-mass energy range from 2.0 to 4.95 GeV, with a peak luminosity of $1 \times 10^{33}\ \text{cm}^{-2}\,\text{s}^{-1}$ achieved at $\sqrt{s} = 3.77$ GeV. BESIII has collected large data samples in this energy region [15,16]. The cylindrical core of the BESIII detector consists of a helium-based main drift chamber (MDC), a plastic scintillator time-of-flight (TOF) system, and a CsI(Tl) electromagnetic calorimeter (EMC), which are all enclosed in a super conducting solenoidal magnet providing a 1.0 T magnetic field. The solenoid is supported by an octagonal flux-return yoke with resistive plate counter modules interleaved with steel for muon identification. The acceptance for charged particles and photons is 93% of the full solid angle, and the charged-particle momentum resolution at 1 GeV/c is 0.5%. The photon energy resolution is 2.5% (5%) at 1.0 GeV in the barrel (end-cap) region. The time resolution in the TOF barrel region is 68 ps, while that in the end-cap region is 110 ps. The end-cap TOF system was upgraded in 2015 using multigap resistive plate chamber technology, providing a time resolution of 60 ps, which benefits ~84% of the data used in this analysis [17–19].

[*]Full author list given at the end of the article.

Simulated data samples produced with a Geant4-based Monte Carlo (MC) package [20], which includes the geometric description of the BESIII detector and the detector response, are used to determine detection efficiencies and to estimate backgrounds. The simulation models the beam-energy spread and initial-state radiation (ISR) in e^+e^- annihilations with the generator KKMC [21,22]. An inclusive MC sample of 2.7 billion $\psi(3686)$ events is used to investigate potential background. The inclusive MC sample includes the production of the $\psi(3686)$ resonance, the ISR production of the J/ψ, and the continuum processes incorporated in KKMC. The known particle decays are modeled with EvtGen [23,24] using branching fractions taken from the Particle Data Group [7], while the remaining unknown decays are estimated with LUNDCHARM [25,26].

To optimize the selection criteria and determine the detection efficiency, the signal MC sample of 2.6×10^6 $\psi(3686) \to \Lambda\bar{\Lambda}\eta'$ events is generated with uniform phase space (PHSP), where the process $\eta' \to \gamma\pi^+\pi^-$ is described according to theoretical models [27,28] that have been validated in previous measurements [29], and the process $\eta' \to \eta\pi^+\pi^-$ is simulated according to the distributions measured in Ref. [30]. The data sample taken at the center of mass (CM) energy of 3.773 GeV, corresponding to an integrated luminosity of $(2916.94 \pm 0.18 \pm 29.17)$ pb^{-1} [31,32], is used to estimate the background events directly from e^+e^- annihilations.

III. EVENT SELECTION

In this analysis, the decay $\psi(3686) \to \Lambda\bar{\Lambda}\eta'$ is selected by reconstructing one $\Lambda\bar{\Lambda}$ pair and one η' meson, where the $\Lambda(\bar{\Lambda})$ candidate is reconstructed by the $p\pi^-(\bar{p}\pi^+)$ decay, and the η' candidate is reconstructed by its two dominant decay modes, $\eta' \to \gamma\pi^+\pi^-$ (Mode I) and $\eta' \to \eta\pi^+\pi^-$ (Mode II). Thus, the reconstructed final states for $\psi(3686) \to \Lambda\bar{\Lambda}\eta'$ are $p\bar{p}\pi^+\pi^-\pi^+\pi^-\gamma$ and $p\bar{p}\pi^+\pi^-\pi^+\pi^-\gamma\gamma$.

The number of charged tracks is required to be more than five. Each track must satisfy $|\cos\theta| < 0.93$, where θ is the polar angle with respect to the beam direction. Each photon candidate is required to have a deposited energy in the EMC more than 25 MeV in the barrel region ($|\cos\theta| < 0.80$) and more than 50 MeV in the end-cap region ($0.86 < |\cos\theta| < 0.92$). To exclude showers arising from charged tracks, the angle between the EMC shower and the position of the closest charged track at the EMC must be greater than 10 degrees as measured from the IP. To suppress electronic noise and showers unrelated to the event, the difference between the EMC time and the event-start time is required to be within [0, 700] ns. At least one photon candidate is required for Mode I, and at least two photon candidates for Mode II.

For each charged track, the information from both the TOF and $\mathrm{d}E/\mathrm{d}x$ are combined to form a particle identification (PID) probability for the π, K, and p hypotheses (Prob(i), $i = \pi$, K, p). A charged track is identified as a pion or proton if its probability is greater than that for any other assignments.

The Λ ($\bar{\Lambda}$) candidate is reconstructed from pairs of (anti) proton and oppositely charged pion tracks fulfilling a secondary vertex fit. Events with at least one Λ and one $\bar{\Lambda}$ candidate are selected. When looping over all combinations of Λ and $\bar{\Lambda}$ candidates, the one with the minimal value of $(M(p\pi^-) - M(\Lambda))^2 + (M(\bar{p}\pi^+) - M(\bar{\Lambda}))^2$ is chosen, where $M(\Lambda)$ ($M(\bar{\Lambda})$) is the known mass of the Λ ($\bar{\Lambda}$) baryon [7]. The remaining charged pions not associated to the $\Lambda(\bar{\Lambda})$ candidates are considered as coming from η' decays, and are required to originate from a region of 10 cm around the interaction point along the beam direction and 1 cm in the plane perpendicular to the beam. The pairs of opposite charged pions are requested to pass a primary vertex fit under the $\pi^+\pi^-\Lambda\bar{\Lambda}$ hypothesis, and that combination with the smallest χ^2 is retained.

To improve the momentum resolution and reduce the background, a kinematic fit is applied to the event candidates. For Mode I, the conservation of the initial-state energy and momentum is required (four constraints); for Mode II, in addition to four-momentum conservation, the invariant mass of the photon pair is constrained to the known η mass. For events with more than one or two photons, respectively for Mode I and Mode II, all the combinations are fitted and that with the best fit quality is selected. We further require the fit quality to satisfy $\chi^2_{4C} < 30$ for Mode I and $\chi^2_{5C} < 40$ for Mode II, a selection that is optimized by maximizing the figure of merit $S/\sqrt{S+B}$, where S is the number of signal MC events obtained from MC simulation and $S + B$ is the number of signal and background events obtained from real data.

Events with candidate η' decays are kept for further analysis, by selecting the invariant-mass signal regions $0.94 < M(\gamma\pi^+\pi^-) < 0.97$ GeV$/c^2$ and $|M(\eta\pi^+\pi^-) - M(\eta')| < 10$ MeV$/c^2$ for Mode I and Mode II, respectively. The invariant-mass distributions $M(p\bar{\pi})$ and $M(\bar{p}\pi^-)$ for the two modes are shown in Figs 1 and 2, where the Λ and $\bar{\Lambda}$ peaks are clearly visible.

For Mode I, the $\Lambda(\bar{\Lambda})$ candidates are selected by requiring $|M(p\pi^-/\bar{p}\pi^+) - M(\Lambda/\bar{\Lambda})| < 6$ MeV$/c^2$. This signal region is indicated by arrows in Fig. 1. In order to remove background events from $\psi(3686) \to \Sigma^0\bar{\Lambda}\pi^+\pi^- +$ c.c., we require $|M(\gamma\Lambda/\gamma\bar{\Lambda}) - M(\Sigma^0/\bar{\Sigma}^0)| > 10$ MeV$/c^2$. The distribution of the recoil mass against the $\pi^+\pi^-$ system, $M_{\rm rec}(\pi^+\pi^-)$, is shown in Fig. 3(a), where the J/ψ peak is visible due to the background events from the $\psi(3686) \to \pi^+\pi^- J/\psi$ process. To veto this background, the recoil mass is required to satisfy $|M_{\rm rec}(\pi^+\pi^-) - M(J/\psi)| > 8$ MeV$/c^2$. The recoil mass against the γ, $M_{\rm rec}(\gamma)$, is shown in Fig. 3(b), where the three visible peaks due to the χ_{c0}, χ_{c1} and χ_{c2} mesons decay into $\pi^\pm\Sigma^{*\mp}\bar{\Lambda}$+c.c.($\Sigma^{*\mp} \to \pi^\mp\Lambda$). To suppress these background

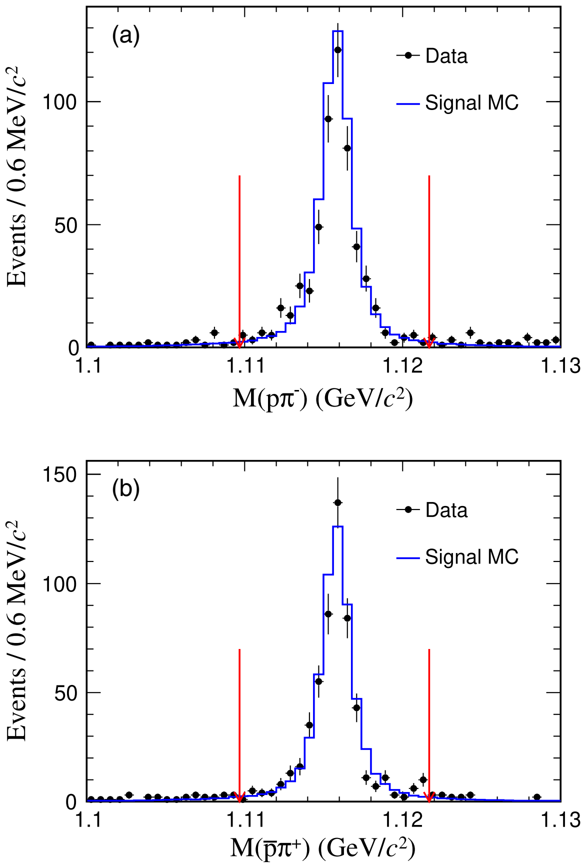

FIG. 1. Distributions of $M_{p\pi^-}$ (a) and $M_{\bar{p}\pi^+}$ (b) for Mode I, where the arrows indicate the region within which the $\Lambda/\bar{\Lambda}$ signal is selected.

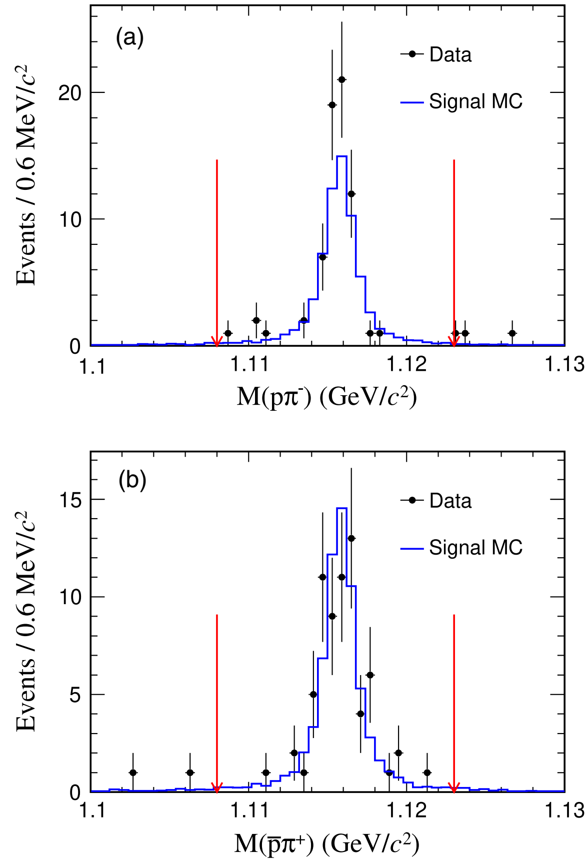

FIG. 2. Distributions of $M_{p\pi^-}$ (a) and $M_{\bar{p}\pi^+}$ (b) for Mode II, where the arrows indicate the region within which the $\Lambda/\bar{\Lambda}$ signal is selected.

events, events in the mass regions $|M_{\rm rec}(\gamma) - M(\chi_{c0})| < 16$ MeV/c^2, $|M_{\rm rec}(\gamma) - M(\chi_{c1})| < 10$ MeV/c^2, and $|M_{\rm rec}(\gamma) - M(\chi_{c2})| < 10$ MeV/c^2 are rejected. The additional requirements $|M(\Lambda\pi^-/\bar{\Lambda}\pi^+) - M(\Xi)| > 0.008$ GeV/c^2 and $|M(\Lambda\pi^-/\bar{\Lambda}\pi^+) - M(\Sigma(1385))| > 0.040$ GeV/c^2 are applied to remove background events with Ξ and $\Sigma(1385)$ baryons in the final states, where $M(X)$ is the known mass of the X particle from Particle Data Group (PDG) [7].

For Mode II, the $\Lambda(\bar{\Lambda})$ candidates are selected by requiring $1.108 < M(p\pi^-/\bar{p}\pi^+) < 1.123$ GeV/c^2. The background events from $\psi(3686) \to \eta J/\psi$ are removed by requiring $|M_{\rm rec}(\gamma\gamma) - M(J/\psi)| > 10$ MeV/c^2, as shown in Fig. 4, where $M_{\rm rec}(\gamma\gamma)$ and $M(J/\psi)$ are the recoil mass against $\gamma\gamma$ and the mass of the J/ψ meson from PDG, respectively.

The $M(\gamma\pi^+\pi^-)$ and $M(\eta\pi^+\pi^-)$ distributions, after these selection requirements, are shown in Figs. 5(a) and (b), where the η' peaks can be seen clearly. To verify that these peaks are not from background events, the distribution of candidates passing the same selection from 2.7 billion inclusive $\psi(3686)$ events are obtained and shown as shaded histograms in Figs. 5(a) and (b); the background events have an approximately flat distribution and do not peak in the η' mass region.

To estimate the number of background events coming directly from e^+e^- annihilation due to quantum electrodynamics processes, which we call QED background, the same analysis is performed on the data samples taken at the CM energy of 3.773 GeV, with an integrated luminosity of $(2916.94 \pm 0.18 \pm 29.17)$ pb^{-1} [31]. For Mode I, several η decays leak into η' signal region in the $M(\gamma\pi^+\pi^-)$ distribution, and are classified as QED background. The number of background events is extracted by fitting the $M(\gamma\pi^+\pi^-)$ distribution, normalized to the $\psi(3686)$ data taking into account the integrated luminosity and energy dependent cross section of the QED processes [33]. The number of QED background events is determined to be

$$N_{\rm bkg} = N_{\psi(3773)} \times \frac{\mathcal{L}_{\psi(3686)}}{\mathcal{L}_{\psi(3773)}} \times \frac{s_{\psi(3773)}}{s_{\psi(3686)}}, \quad (1)$$

where $N_{\psi(3773)}$ is the number of background events obtained from data at the CM energy of 3.773 GeV; $\mathcal{L}_{\psi(3686)}$ and $\mathcal{L}_{\psi(3773)}$ is the integrated luminosity of $\psi(3686)$ and $\psi(3773)$ data samples, respectively, and $\sqrt{s_{\psi(3686)}}$ and $\sqrt{s_{\psi(3773)}}$ are the CM energies of $\psi(3686)$

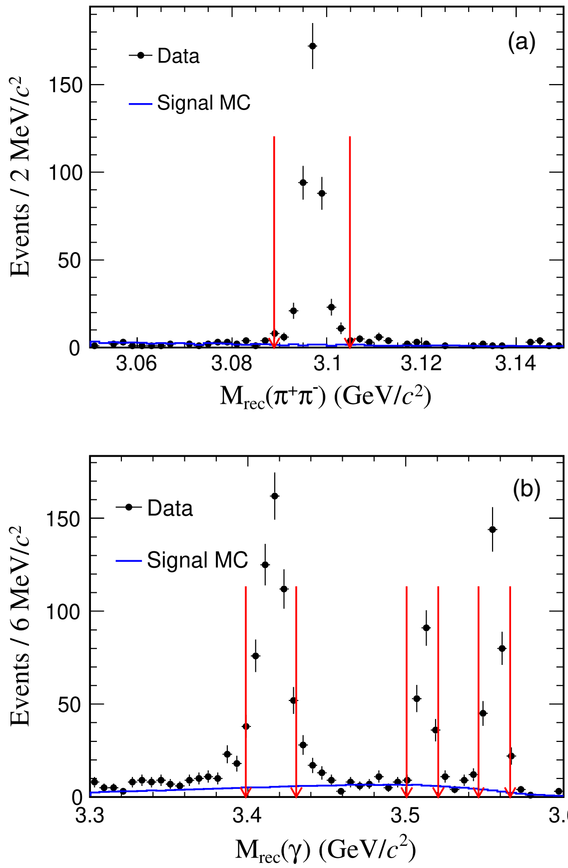

FIG. 3. Distributions of $M_{\rm rec}(\pi^+\pi^-)$ (a) and $M_{\rm rec}(\gamma)$ (b) for Mode I, where the solid arrows indicate the mass window within which (a) J/ψ and (b) $\chi_{c0/c1/c2}$ decays are vetoed. The signal MC is normalized to the measured branching fraction.

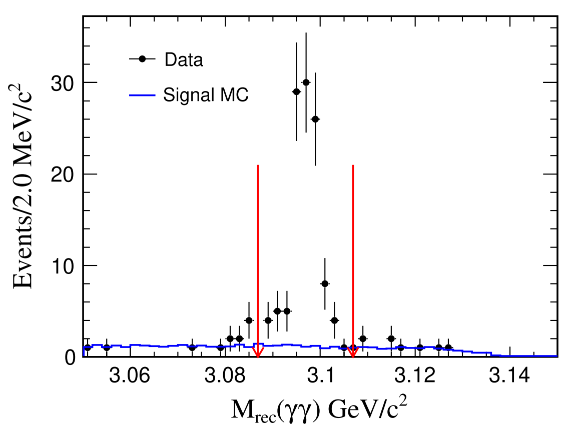

FIG. 4. Distributions of $M_{\rm rec}(\gamma\gamma)$ for Mode II, where the solid arrows indicate the mass window within which J/ψ decays are vetoed. The signal MC is normalized to the measured branching fraction.

and $\psi(3773)$ data samples, respectively. The normalized number of QED background events due to e^+e^- annihilations is 8.1 ± 4.8 for Mode I, which is subtracted in order to determine the signal yield. For Mode II, only 2 events survive after the event selection, which is considered negligible.

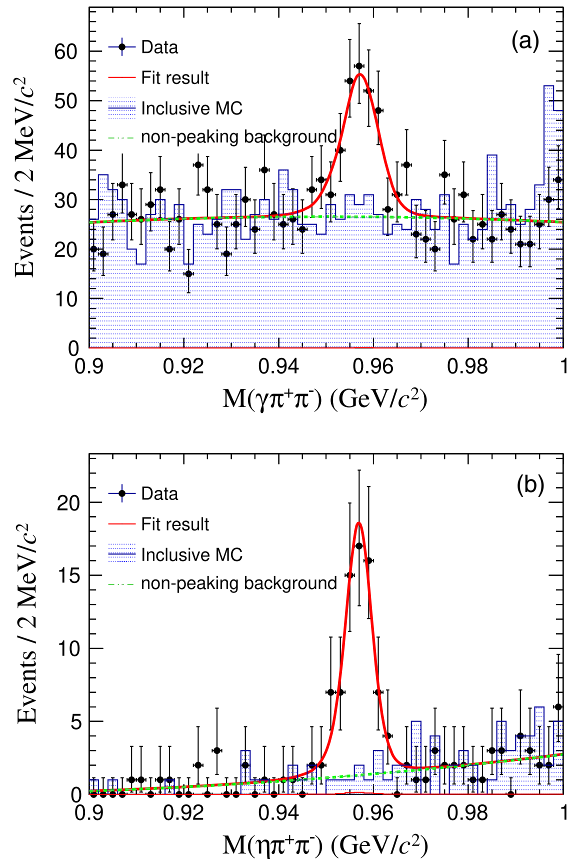

FIG. 5. Distributions of $M(\gamma\pi^+\pi^-)$ (a) and $M(\eta\pi^+\pi^-)$ (b).

IV. BRANCHING FRACTION MEASUREMENT

The $\psi(3686) \to \Lambda\bar{\Lambda}\eta'$ signal yields for Mode I and Mode II are obtained from an extended unbinned maximum likelihood fit to the $M(\gamma\pi^+\pi^-)$ and $M(\eta\pi^+\pi^-)$ distributions, respectively. The total probability density function consists of a signal and a nonpeaking background contribution. The signal component is modeled with the MC signal shape convolved with a Gaussian function to account for a possible difference in the mass resolution between data and MC simulation, and the nonpeaking background is parameterized by a second-order Chebychev polynomial. From the fit results, indicated by the red solid lines in Fig. 5, we obtain 148 ± 24 and 70 ± 10 $\psi(3686) \to \Lambda\bar{\Lambda}\eta'$ events with statistical significances of 6.8σ and 10σ for Mode I and Mode II, respectively. The statistical significance is determined by the change in the log-likelihood value and in the number of degrees of freedom in the fit with and without the η' signal.

To investigate for the presence of possible intermediate structures, we study the background-subtracted $\Lambda\eta'(\bar{\Lambda}\eta')$ mass distributions. For each bin, the number of signal events in data is extracted by fitting the $M(\gamma\pi^+\pi^-)$ and

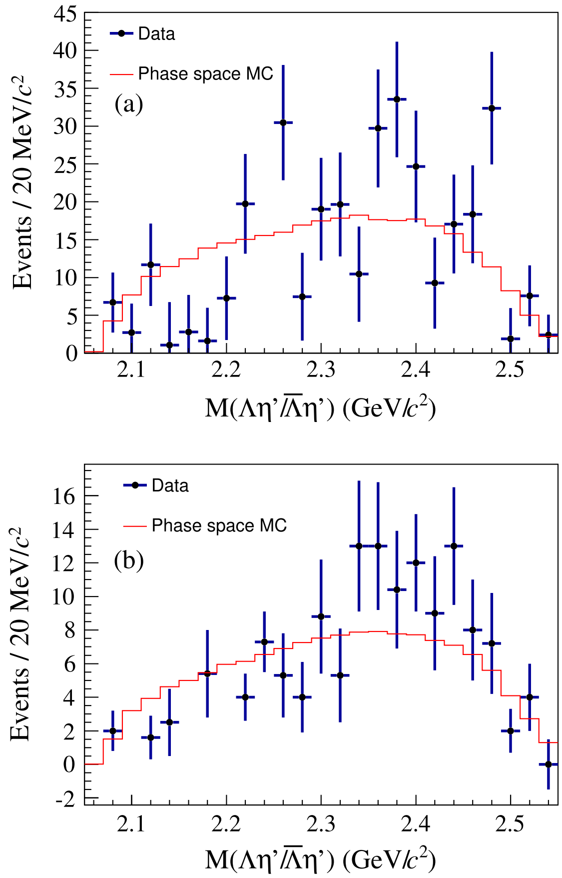

FIG. 6. Distributions of $M_{\Lambda\eta'/\bar{\Lambda}\eta'}$ for Mode I (a) and Mode II (b).

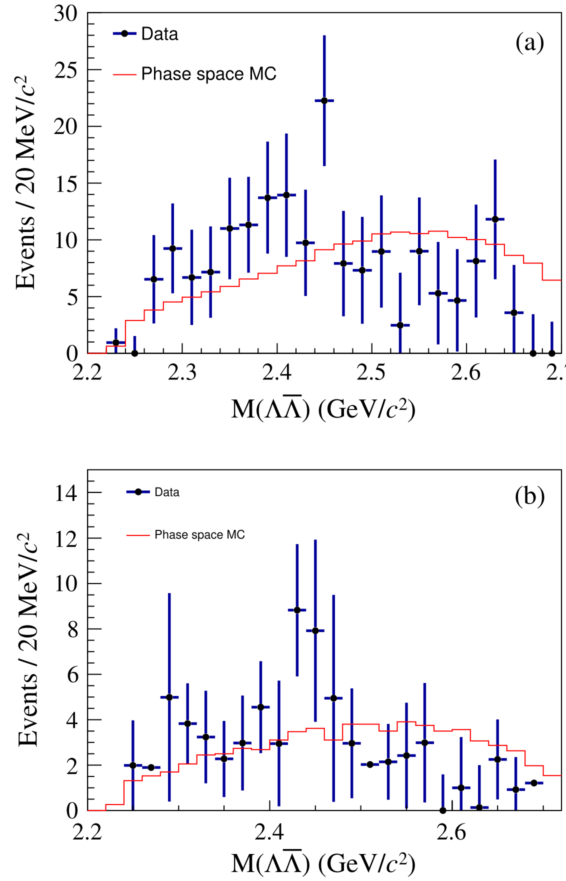

FIG. 7. Distributions of $M_{\Lambda\bar{\Lambda}}$ for Mode I (a) and Mode II (b).

$M(\eta\pi^+\pi^-)$ distributions, respectively, for Mode I and Mode II. The obtained results are shown in Fig. 6, which display no evident structures. Furthermore, the background-subtracted $\Lambda\bar{\Lambda}$ mass distributions with the above similar procedure are shown in Fig. 7, where no structures are observed either.

The detection efficiencies are obtained from MC simulations produced with a uniform phase-space distribution for the three-body decay $\psi(3686) \to \Lambda\bar{\Lambda}\eta'$. The detection efficiencies are determined to be 6.50% and 4.58% for Mode I and Mode II, respectively.

The branching fraction of $\psi(3686) \to \Lambda\bar{\Lambda}\eta'$ is calculated with

$$\mathcal{B}(\psi(3686) \to \Lambda\bar{\Lambda}\eta') = \frac{N_{\mathrm{obs}} - N_{\mathrm{bkg}}}{\mathcal{N}_\psi \mathcal{B}^2(\Lambda \to p\pi^-)\mathcal{B}(\eta' \to X)\varepsilon}, \quad (2)$$

where N_{obs} is the number of observed signal candidates, N_{bkg} is the number of QED background events, $\mathcal{N}_\psi$ is the number of $\psi(3686)$ events [12], ε is the detection efficiency obtained from MC simulation, $\mathcal{B}(\Lambda \to p\pi^-)$ is the branching fraction of $\Lambda \to p\pi^-$ and $\mathcal{B}(\eta' \to X)$ represents the branching fraction of $\eta' \to \gamma\pi^+\pi^-$ or the product branching fraction of $\eta' \to \eta\pi^+\pi^-$ and $\eta \to \gamma\gamma$. The intermediate branching fractions are taken from the PDG [7].

The obtained values of the branching fractions of $\psi(3686) \to \Lambda\bar{\Lambda}\eta'$ are summarized in Table I. The results from the two η' decay modes are consistent with each other within their uncertainties, thus the two measurements are combined, taking accounted of the correlated uncertainties (see Sec. V for details); the mean value and the uncertainty are calculated following the procedure of Ref. [34],

$$\bar{x} \pm \sigma(\bar{x}) = \frac{\Sigma_j(x_j \cdot \Sigma_i w_{ij})}{\Sigma_i\Sigma_j w_{ij}} \pm \sqrt{\frac{1}{\Sigma_i\Sigma_j w_{ij}}}, \quad (3)$$

where i and j are summed over all decay modes, w_{ij} is the element of the weight matrix $W = V_x^{-1}$, and V_x is the covariance error matrix calculated according to the statistical uncertainties and the systematic uncertainties.

TABLE I. The branching fraction results and the values used in the branching fraction calculation for each decay mode, where the first uncertainty is statistical and the second is systematic.

Mode	N_{obs}	N_{bkg}	$\varepsilon(\%)$	$\mathcal{B}$ $(\times 10^{-6})$
I	148 ± 24	8.1 ± 4.8	6.50	$6.59 \pm 1.15 \pm 0.53$
II	70 ± 10		4.58	$8.25 \pm 1.18 \pm 0.67$
Combined				$7.34 \pm 0.94 \pm 0.43$

TABLE II. Relative systematic uncertainties in the branching-fraction measurement (in unit of %). The sources marked "*" are in common for the two η' decay modes.

Sources	Mode I	Mode II
Number of $\psi(3686)$ events*	0.5	0.5
MDC tracking*	2.0	2.0
PID efficiency*	6.0	6.0
Photon detection efficiency	1.0	2.0
$\Lambda(\bar{\Lambda})$ reconstruction*	0.7	0.7
Kinematic fit	0.6	0.6
$\Lambda(\bar{\Lambda})$ intermediate decays		
$\Lambda\to p\pi^-$*	1.6	1.6
$\bar{\Lambda}\to\bar{p}\pi^+$*		
η' intermediate decays		
$\eta'\to\gamma\pi^+\pi^-$	1.4	...
$\eta'\to\eta\pi^+\pi^-$	...	1.2
$\eta\to\gamma\gamma$	...	0.5
Continuum background	3.3	...
Mass spectrum fitting		
Signal shape	0.7	0.7
Background shape	2.0	1.2
Fit range	1.4	3.7
Total	8.0	8.1

When combining the results of the two decay modes, the error matrix is calculated as

$$V=\begin{pmatrix}\sigma_1^2+\epsilon_f^2x_1^2 & \epsilon_f^2x_1x_2\\ \epsilon_f^2x_1x_2 & \sigma_2^2+\epsilon_f^2x_2^2\end{pmatrix}, \qquad (4)$$

where σ_i is the independent absolute uncertainty (the statistical uncertainty and all independent systematical uncertainties are added in quadrature) in the measurement mode i, and ϵ_f is the common relative systematic uncertainty between the two measurements (all the common systematic uncertainties are added in quadrature; the entries in Table II marked with $*$ are the uncertainties in common with the two η' decays while the other uncertainties are different); x_i is the measured value for mode i. The combined branching fraction of $\psi(3686)\to\Lambda\bar{\Lambda}\eta'$ is found to be $(7.34\pm0.94(\mathrm{stat})\pm0.43(\mathrm{sys}))\times10^{-6}$.

V. SYSTEMATIC UNCERTAINTIES

The sources of systematic uncertainties and their corresponding contributions to the measurements of the branching fractions are summarized in Table II. Assuming that all sources are independent, the total systematic uncertainties are obtained by adding the individual contributions in quadrature and are determined to be 8.0% for Mode I and 8.1% for Mode II.

Number of $\psi(3686)$ events: The total number of $\psi(3686)$ events, $(27.12\pm0.14)\times10^8$, is determined by measuring the yield of inclusive hadronic events [12], and its uncertainty is estimated to be 0.5%.

Tracking efficiency: The uncertainty due to differences in the tracking efficiency between data and MC is 1.0% for each charged track coming from a primary vertex, according to a study of $J/\psi\to\rho\pi$ and $J/\psi\to p\bar{p}\pi^+\pi^-$ events [35]. Therefore, the uncertainty from this source associated with the η' reconstruction is 2.0%. The corresponding uncertainty associated with the Λ and $\bar{\Lambda}$ reconstruction is determined separately, and discussed below.

PID efficiency: The PID efficiency has been investigated using a control sample of $J/\psi\to p\bar{p}\pi^+\pi^-$ decays. The uncertainty is assigned to be 1.0% per charged track. In this analysis, all charged tracks must satisfy PID requirements, so the total systematic uncertainty from this source is assigned to be 6.0%.

Photon detection efficiency: The efficiency of the photon reconstruction is studied with a control sample $\psi(3686)\to\pi^+\pi^-J/\psi, J/\psi\to\rho^0\pi^0$ events [36]. The systematic uncertainty in the photon selection is assigned to be 1.0% per photon.

Λ and $\bar{\Lambda}$ reconstruction efficiency: The momentum-dependent $\Lambda(\bar{\Lambda})$ reconstruction efficiency has been studied by calculating the overall tracking efficiency in a given $\cos\theta$ range using a control sample of $J/\psi\to pK^-\bar{\Lambda}+\mathrm{c.c.}$ decays. The difference between data and MC simulation, 0.70%, is taken as the systematic uncertainty.

Kinematic fit: The systematic uncertainty due to the kinematic fit is estimated by correcting the helix parameters of charged tracks according to the method described in Ref. [37]. We take the efficiency from the track-parameter-corrected MC sample as the baseline value, and assign half of the difference in the signal efficiencies before and after the correction as the associated systematic uncertainty, which is 0.6% for both Mode I and Mode II.

Mass window: The uncertainty due to the mass windows used to select signal events or veto backgrounds originates from the differences in the mass resolutions between data and MC simulation. The analysis is repeated with larger and smaller values of the mass window. The maximum relative change in the measured branching fraction is not significant after considering the correlations between the signal yields, hence this uncertainty is considered to be negligible.

Intermediate decays: The systematic uncertainties associated with the knowledge of the branching fractions of the intermediate decays, including $\Lambda\to p\pi^-$, $\eta'\to\gamma\pi^+\pi^-$, $\eta'\to\pi^+\pi^-\eta$ and $\eta\to\gamma\gamma$, are taken from the uncertainties listed in the PDG [7].

Continuum background: The systematic uncertainty associated with the level of continuum background is determined by redetermining the branching fraction after varying the continuum background yield by $\pm1\sigma$ of its statistical uncertainty and assigning the change in branching fraction as the systematic uncertainty.

Signal shape and background shape: To estimate the uncertainty due to the choice of signal shape, the MC-simulated shape convolved with a Gaussian function is replaced by a simple MC shape and the resulting differences in the branching fraction is assigned as the systematic uncertainty. In the case of the background shape, the second-order Chebychev polynomial used for the baseline result is replaced by a first-order or third-order Chebychev polynomial. The largest change of branching fraction is taken as the systematic uncertainty.

Fit range: The uncertainty associated with this source is estimated by varying the fit range as $(0.89, 1.01)$ GeV$/c^2$, $(0.89, 0.99)$ GeV$/c^2$, $(0.91, 1.01)$ GeV$/c^2$ and $(0.91, 0.99)$ GeV$/c^2$, and the maximum resulting difference is assigned as the systematic uncertainty.

VI. SUMMARY

The decay $\psi(3686) \to \Lambda\bar{\Lambda}\eta'$ with the subsequent decay modes $\eta' \to \gamma\pi^+\pi^-$ (Mode I) and $\eta' \to \eta\pi^+\pi^-$ (Mode II) is observed for the first time, using a data sample of $(27.12 \pm 0.14) \times 10^8$ $\psi(3686)$ events. The corresponding branching fractions are measured be $(6.59 \pm 1.15(\mathrm{stat}) \pm 0.53(\mathrm{sys})) \times 10^{-6}$ and $(8.25 \pm 1.18(\mathrm{stat}) \pm 0.67(\mathrm{sys})) \times 10^{-6}$, respectively. The combined branching fraction is $B(\psi(3686) \to \Lambda\bar{\Lambda}\eta') = (7.34 \pm 0.94(\mathrm{stat}) \pm 0.43(\mathrm{sys})) \times 10^{-6}$.

We have also searched for possible excited Λ states and the enhancement near the $\Lambda\bar{\Lambda}$ production, but no evident structure is observed. In the future, a super τ charm factory will collect more data and searches for excited hyperon states will become possible [38].

ACKNOWLEDGMENTS

The BESIII Collaboration thanks the staff of BEPCII and the IHEP computing center for their strong support. This work is supported in part by National Key R&D Program of China under Contracts No. 2020YFA0406300, No. 2020YFA0406400; National Natural Science Foundation of China (NSFC) under Contracts No. 11635010, No. 11735014, No. 11835012, No. 11935015, No. 11935016, No. 11935018, No. 11961141012, No. 12022510, No. 12025502, No. 12035009, No. 12035013, No. 12061131003, No. 12075250, No. 12192260, No. 12192261, No. 12192262, No. 12192263, No. 12192264, No. 12192265, No. 12221005, No. 12225509, No. 12235017; the Chinese Academy of Sciences (CAS) Large-Scale Scientific Facility Program; the CAS Center for Excellence in Particle Physics (CCEPP); Joint Large-Scale Scientific Facility Funds of the NSFC and CAS under Contract No. U1832207; CAS Key Research Program of Frontier Sciences under Contracts No. QYZDJ-SSW-SLH003, No. QYZDJ-SSW-SLH040; 100 Talents Program of CAS; The Institute of Nuclear and Particle Physics (INPAC) and Shanghai Key Laboratory for Particle Physics and Cosmology; European Union's Horizon 2020 research and innovation programme under Marie Sklodowska-Curie grant agreement under Contract No. 894790; German Research Foundation DFG under Contracts Nos. 455635585, Collaborative Research Center CRC 1044, FOR5327, GRK 2149; Istituto Nazionale di Fisica Nucleare, Italy; Ministry of Development of Turkey under Contract No. DPT2006K-120470; National Research Foundation of Korea under Contract No. NRF-2022R1A2C1092335; National Science and Technology fund of Mongolia; National Science Research and Innovation Fund (NSRF) via the Program Management Unit for Human Resources & Institutional Development, Research and Innovation of Thailand under Contract No. B16F640076; Polish National Science Centre under Contract No. 2019/35/O/ST2/02907; The Swedish Research Council; U.S. Department of Energy under Contract No. DE-FG02-05ER41374.

[1] W. Kwong, J. L. Rosner, and C. Quigg, Annu. Rev. Nucl. Part. Sci. **37**, 325 (1987).
[2] E. Eichten, S. Godfrey, H. Mahlke, and J. L. Rosner, Rev. Mod. Phys. **80**, 1161 (2008).
[3] R. Sinha and S. Okubo, Phys. Rev. D **30**, 2333 (1984).
[4] M. Ablikim *et al.* (BESIII Collaboration), Phys. Rev. D **99**, 032006 (2019).
[5] K. Zhu, X. H. Mo, and C. Z. Yuan, Int. J. Mod. Phys. A **30**, 1550148 (2015).
[6] D. M. Manley *et al.* (Crystal Ball Collaboration), Phys. Rev. Lett. **88**, 012002 (2001).
[7] R. L. Workman *et al.* (Particle Data Group), Prog. Theor. Exp. Phys. **2022**, 083C01 (2022).
[8] M. Ablikim *et al.* (BESIII Collaboration), Phys. Rev. D **106**, 072006 (2022).
[9] M. Ablikim *et al.* (BESIII Collaboration), Phys. Rev. D **87**, 052007 (2013).
[10] A. V. Sarantsev, M. Matveev, V. A. Nikonov, A. V. Anisovich, U. Thoma, and E. Klempt, Eur. Phys. J. A **55**, 180 (2019).
[11] Volker Crede, AIP Conf. Proc. **2249**, 020003 (2020).
[12] M. Ablikim *et al.* (BESIII Collaboration), Chin. Phys. C **42**, 023001 (2018). With the same approach as for $\psi(3686)$ events taken in 2009, the preliminary number of $\psi(3686)$ events taken in 2009, 2012, and 2021 is determined to be 27.12×10^8 with an uncertainty of 0.5%.

[13] M. Ablikim *et al.* (BESIII Collaboration), Nucl. Instrum. Methods Phys. Res., Sect. A **614**, 345 (2010).
[14] C. H. Yu *et al.*, *Proceedings of IPAC2016, Busan, Korea* (2016), http://jacow.org/ipac2016/papers/tuya01.pdf.
[15] M. Ablikim *et al.* (BESIII Collaboration), Chin. Phys. C **44**, 040001 (2020).
[16] J. W. Zhang, L. H. Wu, S. S. Sun *et al.*, Radiat. Detect. Technol. Methods **6**, 289 (2022).
[17] X. Li *et al.*, Radiat. Detect. Technol. Methods **1**, 13 (2017).
[18] Y. X. Guo *et al.*, Radiat. Detect. Technol. Methods **1**, 15 (2017).
[19] P. Cao *et al.*, Nucl. Instrum. Methods Phys. Res., Sect. A **953**, 163053 (2020).
[20] S. Agostinelli *et al.* (GEANT4 Collaboration), Nucl. Instrum. Methods Phys. Res., Sect. A **506**, 250 (2003).
[21] S. Jadach and B. F. L. Ward, and Z. Was, Comput. Phys. Commun. **130**, 260 (2000).
[22] S. Jadach, B. F. L. Ward, and Z. Was, Phys. Rev. D **63**, 113009 (2001).
[23] D. J. Lange, Nucl. Instrum. Methods Phys. Res., Sect. A **462**, 152 (2001).
[24] R. G. Ping, Chin. Phys. C **32**, 599 (2008).
[25] J. C. Chen, G. S. Huang, X. R. Qi, D. H. Zhang, and Y. S. Zhu, Phys. Rev. D **62**, 034003 (2000).
[26] R. L. Yang, R. G. Ping, and H. Chen, Chin. Phys. Lett. **31**, 061301 (2014).
[27] J. Wess and B. Zumino, Phys. Lett. **37B**, 95 (1971).
[28] E. Witten, Nucl. Phys. **B223**, 422 (1983).
[29] M. Ablikim *et al.* (BESIII Collaboration), Phys. Rev. Lett. **120**, 242003 (2018).
[30] M. Ablikim *et al.* (BESIII Collaboration), Phys. Rev. D **97**, 012003 (2018).
[31] M. Ablikim *et al.* (BESIII Collaboration), Chin. Phys. C **37**, 123001 (2013).
[32] M. Ablikim *et al.* (BESIII Collaboration), Phys. Lett. B **753**, 629 (2016).
[33] M. Ablikim *et al.* (BESIII Collaboration), Chin. Phys. C **36**, 915 (2012).
[34] G. D'Agostini, Nucl. Instrum. Methods Phys. Res., Sect. A **346**, 306 (1994).
[35] M. Ablikim *et al.* (BESIII Collaboration), Phys. Rev. D **85**, 092012 (2012).
[36] M. Ablikim *et al.* (BESIII Collaboration), Phys. Rev. D **83**, 112005 (2011).
[37] M. Ablikim *et al.* (BESIII Collaboration), Phys. Rev. D **87**, 012002 (2013).
[38] M. Achasov *et al.*, arXiv:2303.15790.

M. Ablikim,[1] M. N. Achasov,[5,b] P. Adlarson,[75] X. C. Ai,[81] R. Aliberti,[36] A. Amoroso,[74a,74c] M. R. An,[40] Q. An,[71,58] Y. Bai,[57] O. Bakina,[37] I. Balossino,[30a] Y. Ban,[47,g] V. Batozskaya,[1,45] K. Begzsuren,[33] N. Berger,[36] M. Berlowski,[45] M. Bertani,[29a] D. Bettoni,[30a] F. Bianchi,[74a,74c] E. Bianco,[74a,74c] A. Bortone,[74a,74c] I. Boyko,[37] R. A. Briere,[6] A. Brueggemann,[68] H. Cai,[76] X. Cai,[1,58] A. Calcaterra,[29a] G. F. Cao,[1,63] N. Cao,[1,63] S. A. Cetin,[62a] J. F. Chang,[1,58] T. T. Chang,[77] W. L. Chang,[1,63] G. R. Che,[44] G. Chelkov,[37,a] C. Chen,[44] Chao Chen,[55] G. Chen,[1] H. S. Chen,[1,63] M. L. Chen,[1,58,63] S. J. Chen,[43] S. L. Chen,[46] S. M. Chen,[61] T. Chen,[1,63] X. R. Chen,[32,63] X. T. Chen,[1,63] Y. B. Chen,[1,58] Y. Q. Chen,[35] Z. J. Chen,[26,h] W. S. Cheng,[74c] S. K. Choi,[11] X. Chu,[44] G. Cibinetto,[30a] S. C. Coen,[4] F. Cossio,[74c] J. J. Cui,[50] H. L. Dai,[1,58] J. P. Dai,[79] A. Dbeyssi,[19] R. E. de Boer,[4] D. Dedovich,[37] Z. Y. Deng,[1] A. Denig,[36] I. Denysenko,[37] M. Destefanis,[74a,74c] F. De Mori,[74a,74c] B. Ding,[66,1] X. X. Ding,[47,g] Y. Ding,[41] Y. Ding,[35] J. Dong,[1,58] L. Y. Dong,[1,63] M. Y. Dong,[1,58,63] X. Dong,[76] M. C. Du,[1] S. X. Du,[81] Z. H. Duan,[43] P. Egorov,[37,a] Y. H. Fan,[46] J. Fang,[1,58] S. S. Fang,[1,63] W. X. Fang,[1] Y. Fang,[1] R. Farinelli,[30a] L. Fava,[74b,74c] F. Feldbauer,[4] G. Felici,[29a] C. Q. Feng,[71,58] J. H. Feng,[59] K. Fischer,[69] M. Fritsch,[4] C. D. Fu,[1] J. L. Fu,[63] Y. W. Fu,[1] H. Gao,[63] Y. N. Gao,[47,g] Yang Gao,[71,58] S. Garbolino,[74c] I. Garzia,[30a,30b] P. T. Ge,[76] Z. W. Ge,[43] C. Geng,[59] E. M. Gersabeck,[67] A. Gilman,[69] K. Goetzen,[14] L. Gong,[41] W. X. Gong,[1,58] W. Gradl,[36] S. Gramigna,[30a,30b] M. Greco,[74a,74c] M. H. Gu,[1,58] Y. T. Gu,[16] C. Y. Guan,[1,63] Z. L. Guan,[23] A. Q. Guo,[32,63] L. B. Guo,[42] M. J. Guo,[50] R. P. Guo,[49] Y. P. Guo,[13,f] A. Guskov,[37,a] T. T. Han,[50] W. Y. Han,[40] X. Q. Hao,[20] F. A. Harris,[65] K. K. He,[55] K. L. He,[1,63] F. H. H. Heinsius,[4] C. H. Heinz,[36] Y. K. Heng,[1,58,63] C. Herold,[60] T. Holtmann,[4] P. C. Hong,[13,f] G. Y. Hou,[1,63] X. T. Hou,[1,63] Y. R. Hou,[63] Z. L. Hou,[1] H. M. Hu,[1,63] J. F. Hu,[56,i] T. Hu,[1,58,63] Y. Hu,[1] G. S. Huang,[71,58] K. X. Huang,[59] L. Q. Huang,[32,63] X. T. Huang,[50] Y. P. Huang,[1] T. Hussain,[73] N. Hüsken,[28,36] N. in der Wiesche,[68] J. Jackson,[28] S. Jaeger,[4] S. Janchiv,[33] J. H. Jeong,[11] Q. Ji,[1] Q. P. Ji,[20] X. B. Ji,[1,63] X. L. Ji,[1,58] Y. Y. Ji,[50] X. Q. Jia,[50] Z. K. Jia,[71,58] H. J. Jiang,[76] P. C. Jiang,[47,g] S. S. Jiang,[40] T. J. Jiang,[17] X. S. Jiang,[1,58,63] Y. Jiang,[63] J. B. Jiao,[50] Z. Jiao,[24] S. Jin,[43] Y. Jin,[66] M. Q. Jing,[1,63] T. Johansson,[75] X. K.,[1] S. Kabana,[34] N. Kalantar-Nayestanaki,[64] X. L. Kang,[10] X. S. Kang,[41] M. Kavatsyuk,[64] B. C. Ke,[81] A. Khoukaz,[68] R. Kiuchi,[1] R. Kliemt,[14] O. B. Kolcu,[62a] B. Kopf,[4] M. Kuessner,[4] A. Kupsc,[45,75] W. Kühn,[38] J. J. Lane,[67] P. Larin,[19] A. Lavania,[27] L. Lavezzi,[74a,74c] T. T. Lei,[71,58] Z. H. Lei,[71,58] H. Leithoff,[36] M. Lellmann,[36] T. Lenz,[36] C. Li,[48] C. Li,[44] C. H. Li,[40] Cheng Li,[71,58] D. M. Li,[81] F. Li,[1,58] G. Li,[1] H. Li,[71,58] H. B. Li,[1,63] H. J. Li,[20] H. N. Li,[56,i] Hui Li,[44] J. R. Li,[61] J. S. Li,[59] J. W. Li,[50] K. L. Li,[20] Ke Li,[1] L. J. Li,[1,63] L. K. Li,[1] Lei Li,[3] M. H. Li,[44] P. R. Li,[39,j,k] Q. X. Li,[50] S. X. Li,[13] T. Li,[50] W. D. Li,[1,63] W. G. Li,[1] X. H. Li,[71,58] X. L. Li,[50] Xiaoyu Li,[1,63] Y. G. Li,[47,g] Z. J. Li,[59] Z. X. Li,[16] C. Liang,[43] H. Liang,[1,63] H. Liang,[35] H. Liang,[71,58] Y. F. Liang,[54]

Y. T. Liang,[32,63] G. R. Liao,[15] L. Z. Liao,[50] Y. P. Liao,[1,63] J. Libby,[27] A. Limphirat,[60] D. X. Lin,[32,63] T. Lin,[1] B. J. Liu,[1] B. X. Liu,[76] C. Liu,[35] C. X. Liu,[1] F. H. Liu,[53] Fang Liu,[1] Feng Liu,[7] G. M. Liu,[56,i] H. Liu,[39,j,k] H. B. Liu,[16] H. M. Liu,[1,63] Huanhuan Liu,[1] Huihui Liu,[22] J. B. Liu,[71,58] J. L. Liu,[72] J. Y. Liu,[1,63] K. Liu,[1] K. Y. Liu,[41] Ke Liu,[23] L. Liu,[71,58] L. C. Liu,[44] Lu Liu,[44] M. H. Liu,[13,f] P. L. Liu,[1] Q. Liu,[63] S. B. Liu,[71,58] T. Liu,[13,f] W. K. Liu,[44] W. M. Liu,[71,58] X. Liu,[39,j,k] Y. Liu,[81] Y. Liu,[39,j,k] Y. B. Liu,[44] Z. A. Liu,[1,58,63] Z. Q. Liu,[50] X. C. Lou,[1,58,63] F. X. Lu,[59] H. J. Lu,[24] J. G. Lu,[1,58] X. L. Lu,[1] Y. Lu,[8] Y. P. Lu,[1,58] Z. H. Lu,[1,63] C. L. Luo,[42] M. X. Luo,[80] T. Luo,[13,f] X. L. Luo,[1,58] X. R. Lyu,[63] Y. F. Lyu,[44] F. C. Ma,[41] H. L. Ma,[1] J. L. Ma,[1,63] L. L. Ma,[50] M. M. Ma,[1,63] Q. M. Ma,[1] R. Q. Ma,[1,63] R. T. Ma,[63] X. Y. Ma,[1,58] Y. Ma,[47,g] Y. M. Ma,[32] F. E. Maas,[19] M. Maggiora,[74a,74c] S. Malde,[69] Q. A. Malik,[73] A. Mangoni,[29b] Y. J. Mao,[47,g] Z. P. Mao,[1] S. Marcello,[74a,74c] Z. X. Meng,[66] J. G. Messchendorp,[14,64] G. Mezzadri,[30a] H. Miao,[1,63] T. J. Min,[43] R. E. Mitchell,[28] X. H. Mo,[1,58,63] N. Yu. Muchnoi,[5,b] J. Muskalla,[36] Y. Nefedov,[37] F. Nerling,[19,d] I. B. Nikolaev,[5,b] Z. Ning,[1,58] S. Nisar,[12,l] Q. L. Niu,[39,j,k] W. D. Niu,[55] Y. Niu,[50] S. L. Olsen,[63] Q. Ouyang,[1,58,63] S. Pacetti,[29b,29c] X. Pan,[55] Y. Pan,[57] A. Pathak,[35] P. Patteri,[29a] Y. P. Pei,[71,58] M. Pelizaeus,[4] H. P. Peng,[71,58] Y. Y. Peng,[39,j,k] K. Peters,[14,d] J. L. Ping,[42] R. G. Ping,[1,63] S. Plura,[36] V. Prasad,[34] F. Z. Qi,[1] H. Qi,[71,58] H. R. Qi,[61] M. Qi,[43] T. Y. Qi,[13,f] S. Qian,[1,58] W. B. Qian,[63] C. F. Qiao,[63] J. J. Qin,[72] L. Q. Qin,[15] X. P. Qin,[13,f] X. S. Qin,[50] Z. H. Qin,[1,58] J. F. Qiu,[1] S. Q. Qu,[61] C. F. Redmer,[36] K. J. Ren,[40] A. Rivetti,[74c] M. Rolo,[74c] G. Rong,[1,63] Ch. Rosner,[19] S. N. Ruan,[44] N. Salone,[45] A. Sarantsev,[37,c] Y. Schelhaas,[36] K. Schoenning,[75] M. Scodeggio,[30a,30b] K. Y. Shan,[13,f] W. Shan,[25] X. Y. Shan,[71,58] J. F. Shangguan,[55] L. G. Shao,[1,63] M. Shao,[71,58] C. P. Shen,[13,f] H. F. Shen,[1,63] W. H. Shen,[63] X. Y. Shen,[1,63] B. A. Shi,[63] H. C. Shi,[71,58] J. L. Shi,[13] J. Y. Shi,[1] Q. Q. Shi,[55] R. S. Shi,[1,63] X. Shi,[1,58] J. J. Song,[20] T. Z. Song,[59] W. M. Song,[35,1] Y. J. Song,[13] Y. X. Song,[47,g] S. Sosio,[74a,74c] S. Spataro,[74a,74c] F. Stieler,[36] Y. J. Su,[63] G. B. Sun,[76] G. X. Sun,[1] H. Sun,[63] H. K. Sun,[1] J. F. Sun,[20] K. Sun,[61] L. Sun,[76] S. S. Sun,[1,63] T. Sun,[1,63] W. Y. Sun,[35] Y. Sun,[10] Y. J. Sun,[71,58] Y. Z. Sun,[1] Z. T. Sun,[50] Y. X. Tan,[71,58] C. J. Tang,[54] G. Y. Tang,[1] J. Tang,[59] Y. A. Tang,[76] L. Y. Tao,[72] Q. T. Tao,[26,h] M. Tat,[69] J. X. Teng,[71,58] V. Thoren,[75] W. H. Tian,[52] W. H. Tian,[59] Y. Tian,[32,63] Z. F. Tian,[76] I. Uman,[62b] S. J. Wang,[50] B. Wang,[1] B. L. Wang,[63] Bo Wang,[71,58] C. W. Wang,[43] D. Y. Wang,[47,g] F. Wang,[72] H. J. Wang,[39,j,k] H. P. Wang,[1,63] J. P. Wang,[50] K. Wang,[1,58] L. L. Wang,[1] M. Wang,[50] Meng Wang,[1,63] S. Wang,[13,f] S. Wang,[39,j,k] T. Wang,[13,f] T. J. Wang,[44] W. Wang,[72] W. Wang,[59] W. P. Wang,[71,58] X. Wang,[47,g] X. F. Wang,[39,j,k] X. J. Wang,[40] X. L. Wang,[13,f] Y. Wang,[61] Y. D. Wang,[46] Y. F. Wang,[1,58,63] Y. H. Wang,[48] Y. N. Wang,[46] Y. Q. Wang,[1] Yaqian Wang,[18,1] Yi Wang,[61] Z. Wang,[1,58] Z. L. Wang,[72] Z. Y. Wang,[1,63] Ziyi Wang,[63] D. Wei,[70] D. H. Wei,[15] F. Weidner,[68] S. P. Wen,[1] C. W. Wenzel,[4] U. Wiedner,[4] G. Wilkinson,[69] M. Wolke,[75] L. Wollenberg,[4] C. Wu,[40] J. F. Wu,[1,63] L. H. Wu,[1] L. J. Wu,[1,63] X. Wu,[13,f] X. H. Wu,[35] Y. Wu,[71] Y. H. Wu,[55] Y. J. Wu,[32] Z. Wu,[1,58] L. Xia,[71,58] X. M. Xian,[40] T. Xiang,[47,g] D. Xiao,[39,j,k] G. Y. Xiao,[43] S. Y. Xiao,[1] Y. L. Xiao,[13,f] Z. J. Xiao,[42] C. Xie,[43] X. H. Xie,[47,g] Y. Xie,[50] Y. G. Xie,[1,58] Y. H. Xie,[7] Z. P. Xie,[71,58] T. Y. Xing,[1,63] C. F. Xu,[1,63] C. J. Xu,[59] G. F. Xu,[1] H. Y. Xu,[66] Q. J. Xu,[17] Q. N. Xu,[31] W. Xu,[1,63] W. L. Xu,[66] X. P. Xu,[55] Y. C. Xu,[78] Z. P. Xu,[43] Z. S. Xu,[63] F. Yan,[13,f] L. Yan,[13,f] W. B. Yan,[71,58] W. C. Yan,[81] X. Q. Yan,[1] H. J. Yang,[51,e] H. L. Yang,[35] H. X. Yang,[1] Tao Yang,[1] Y. Yang,[13,f] Y. F. Yang,[44] Y. X. Yang,[1,63] Yifan Yang,[1,63] Z. W. Yang,[39,j,k] Z. P. Yao,[50] M. Ye,[1,58] M. H. Ye,[9] J. H. Yin,[1] Z. Y. You,[59] B. X. Yu,[1,58,63] C. X. Yu,[44] G. Yu,[1,63] J. S. Yu,[26,h] T. Yu,[72] X. D. Yu,[47,g] C. Z. Yuan,[1,63] L. Yuan,[2] S. C. Yuan,[1] X. Q. Yuan,[1] Y. Yuan,[1,63] Z. Y. Yuan,[59] C. X. Yue,[40] A. A. Zafar,[73] F. R. Zeng,[50] X. Zeng,[13,f] Y. Zeng,[26,h] Y. J. Zeng,[1,63] X. Y. Zhai,[35] Y. C. Zhai,[50] Y. H. Zhan,[59] A. Q. Zhang,[1,63] B. L. Zhang,[1,63] B. X. Zhang,[1] D. H. Zhang,[44] G. Y. Zhang,[20] H. Zhang,[71] H. H. Zhang,[35] H. H. Zhang,[59] H. Q. Zhang,[1,58,63] H. Y. Zhang,[1,58] J. Zhang,[81] J. J. Zhang,[52] J. L. Zhang,[21] J. Q. Zhang,[42] J. W. Zhang,[1,58,63] J. X. Zhang,[39,j,k] J. Y. Zhang,[1] J. Z. Zhang,[1,63] Jianyu Zhang,[63] Jiawei Zhang,[1,63] L. M. Zhang,[61] L. Q. Zhang,[59] Lei Zhang,[43] P. Zhang,[1,63] Q. Y. Zhang,[40,81] Shuihan Zhang,[1,63] Shulei Zhang,[26,h] X. D. Zhang,[46] X. M. Zhang,[1] X. Y. Zhang,[50] Xuyan Zhang,[55] Y. Zhang,[69] Y. Zhang,[72] Y. T. Zhang,[81] Y. H. Zhang,[1,58] Yan Zhang,[71,58] Yao Zhang,[1] Z. H. Zhang,[1] Z. L. Zhang,[35] Z. Y. Zhang,[44] Z. Y. Zhang,[76] G. Zhao,[1] J. Zhao,[40] J. Y. Zhao,[1,63] J. Z. Zhao,[1,58] Lei Zhao,[71,58] Ling Zhao,[1] M. G. Zhao,[44] S. J. Zhao,[81] Y. B. Zhao,[1,58] Y. X. Zhao,[32,63] Z. G. Zhao,[71,58] A. Zhemchugov,[37,a] B. Zheng,[72] J. P. Zheng,[1,58] W. J. Zheng,[1,63] Y. H. Zheng,[63] B. Zhong,[42] X. Zhong,[59] H. Zhou,[50] L. P. Zhou,[1,63] X. Zhou,[76] X. K. Zhou,[7] X. R. Zhou,[71,58] X. Y. Zhou,[40] Y. Z. Zhou,[13,f] J. Zhu,[44] K. Zhu,[1] K. J. Zhu,[1,58,63] L. Zhu,[35] L. X. Zhu,[63] S. H. Zhu,[70] S. Q. Zhu,[43] T. J. Zhu,[13,f] W. J. Zhu,[13,f] Y. C. Zhu,[71,58] Z. A. Zhu,[1,63] J. H. Zou,[1] and J. Zu[71,58]

(BESIII Collaboration)

[1]Institute of High Energy Physics, Beijing 100049, People's Republic of China
[2]Beihang University, Beijing 100191, People's Republic of China
[3]Beijing Institute of Petrochemical Technology, Beijing 102617, People's Republic of China
[4]Bochum Ruhr-University, D-44780 Bochum, Germany
[5]Budker Institute of Nuclear Physics SB RAS (BINP), Novosibirsk 630090, Russia
[6]Carnegie Mellon University, Pittsburgh, Pennsylvania 15213, USA
[7]Central China Normal University, Wuhan 430079, People's Republic of China
[8]Central South University, Changsha 410083, People's Republic of China
[9]China Center of Advanced Science and Technology, Beijing 100190, People's Republic of China
[10]China University of Geosciences, Wuhan 430074, People's Republic of China
[11]Chung-Ang University, Seoul, 06974, Republic of Korea
[12]COMSATS University Islamabad, Lahore Campus, Defence Road, Off Raiwind Road, 54000 Lahore, Pakistan
[13]Fudan University, Shanghai 200433, People's Republic of China
[14]GSI Helmholtzcentre for Heavy Ion Research GmbH, D-64291 Darmstadt, Germany
[15]Guangxi Normal University, Guilin 541004, People's Republic of China
[16]Guangxi University, Nanning 530004, People's Republic of China
[17]Hangzhou Normal University, Hangzhou 310036, People's Republic of China
[18]Hebei University, Baoding 071002, People's Republic of China
[19]Helmholtz Institute Mainz, Staudinger Weg 18, D-55099 Mainz, Germany
[20]Henan Normal University, Xinxiang 453007, People's Republic of China
[21]Henan University, Kaifeng 475004, People's Republic of China
[22]Henan University of Science and Technology, Luoyang 471003, People's Republic of China
[23]Henan University of Technology, Zhengzhou 450001, People's Republic of China
[24]Huangshan College, Huangshan 245000, People's Republic of China
[25]Hunan Normal University, Changsha 410081, People's Republic of China
[26]Hunan University, Changsha 410082, People's Republic of China
[27]Indian Institute of Technology Madras, Chennai 600036, India
[28]Indiana University, Bloomington, Indiana 47405, USA
[29a]INFN Laboratori Nazionali di Frascati, I-00044, Frascati, Italy
[29b]INFN Sezione di Perugia, I-06100, Perugia, Italy
[29c]University of Perugia, I-06100, Perugia, Italy
[30a]INFN Sezione di Ferrara, I-44122, Ferrara, Italy
[30b]University of Ferrara, I-44122, Ferrara, Italy
[31]Inner Mongolia University, Hohhot 010021, People's Republic of China
[32]Institute of Modern Physics, Lanzhou 730000, People's Republic of China
[33]Institute of Physics and Technology, Peace Avenue 54B, Ulaanbaatar 13330, Mongolia
[34]Instituto de Alta Investigación, Universidad de Tarapacá, Casilla 7D, Arica 1000000, Chile
[35]Jilin University, Changchun 130012, People's Republic of China
[36]Johannes Gutenberg University of Mainz, Johann-Joachim-Becher-Weg 45, D-55099 Mainz, Germany
[37]Joint Institute for Nuclear Research, 141980 Dubna, Moscow region, Russia
[38]Justus-Liebig-Universitaet Giessen, II. Physikalisches Institut, Heinrich-Buff-Ring 16, D-35392 Giessen, Germany
[39]Lanzhou University, Lanzhou 730000, People's Republic of China
[40]Liaoning Normal University, Dalian 116029, People's Republic of China
[41]Liaoning University, Shenyang 110036, People's Republic of China
[42]Nanjing Normal University, Nanjing 210023, People's Republic of China
[43]Nanjing University, Nanjing 210093, People's Republic of China
[44]Nankai University, Tianjin 300071, People's Republic of China
[45]National Centre for Nuclear Research, Warsaw 02-093, Poland
[46]North China Electric Power University, Beijing 102206, People's Republic of China
[47]Peking University, Beijing 100871, People's Republic of China
[48]Qufu Normal University, Qufu 273165, People's Republic of China
[49]Shandong Normal University, Jinan 250014, People's Republic of China
[50]Shandong University, Jinan 250100, People's Republic of China
[51]Shanghai Jiao Tong University, Shanghai 200240, People's Republic of China
[52]Shanxi Normal University, Linfen 041004, People's Republic of China
[53]Shanxi University, Taiyuan 030006, People's Republic of China
[54]Sichuan University, Chengdu 610064, People's Republic of China
[55]Soochow University, Suzhou 215006, People's Republic of China

[56]*South China Normal University, Guangzhou 510006, People's Republic of China*
[57]*Southeast University, Nanjing 211100, People's Republic of China*
[58]*State Key Laboratory of Particle Detection and Electronics, Beijing 100049, Hefei 230026, People's Republic of China*
[59]*Sun Yat-Sen University, Guangzhou 510275, People's Republic of China*
[60]*Suranaree University of Technology, University Avenue 111, Nakhon Ratchasima 30000, Thailand*
[61]*Tsinghua University, Beijing 100084, People's Republic of China*
[62a]*Turkish Accelerator Center Particle Factory Group, Istinye University, 34010, Istanbul, Turkey*
[62b]*Turkish Accelerator Center Particle Factory Group, Near East University, Nicosia, North Cyprus, 99138, Mersin 10, Turkey*
[63]*University of Chinese Academy of Sciences, Beijing 100049, People's Republic of China*
[64]*University of Groningen, NL-9747 AA Groningen, The Netherlands*
[65]*University of Hawaii, Honolulu, Hawaii 96822, USA*
[66]*University of Jinan, Jinan 250022, People's Republic of China*
[67]*University of Manchester, Oxford Road, Manchester, M13 9PL, United Kingdom*
[68]*University of Muenster, Wilhelm-Klemm-Strasse 9, 48149 Muenster, Germany*
[69]*University of Oxford, Keble Road, Oxford OX13RH, United Kingdom*
[70]*University of Science and Technology Liaoning, Anshan 114051, People's Republic of China*
[71]*University of Science and Technology of China, Hefei 230026, People's Republic of China*
[72]*University of South China, Hengyang 421001, People's Republic of China*
[73]*University of the Punjab, Lahore-54590, Pakistan*
[74a]*University of Turin, I-10125, Turin, Italy*
[74b]*University of Eastern Piedmont, I-15121, Alessandria, Italy*
[74c]*INFN, I-10125, Turin, Italy*
[75]*Uppsala University, Box 516, SE-75120 Uppsala, Sweden*
[76]*Wuhan University, Wuhan 430072, People's Republic of China*
[77]*Xinyang Normal University, Xinyang 464000, People's Republic of China*
[78]*Yantai University, Yantai 264005, People's Republic of China*
[79]*Yunnan University, Kunming 650500, People's Republic of China*
[80]*Zhejiang University, Hangzhou 310027, People's Republic of China*
[81]*Zhengzhou University, Zhengzhou 450001, People's Republic of China*

[a]Also at the Moscow Institute of Physics and Technology, Moscow 141700, Russia.
[b]Also at the Novosibirsk State University, Novosibirsk, 630090, Russia.
[c]Also at the NRC "Kurchatov Institute", PNPI, 188300, Gatchina, Russia.
[d]Also at Goethe University Frankfurt, 60323 Frankfurt am Main, Germany.
[e]Also at Key Laboratory for Particle Physics, Astrophysics and Cosmology, Ministry of Education; Shanghai Key Laboratory for Particle Physics and Cosmology; Institute of Nuclear and Particle Physics, Shanghai 200240, People's Republic of China.
[f]Also at Key Laboratory of Nuclear Physics and Ion-beam Application (MOE) and Institute of Modern Physics, Fudan University, Shanghai 200443, People's Republic of China.
[g]Also at State Key Laboratory of Nuclear Physics and Technology, Peking University, Beijing 100871, People's Republic of China.
[h]Also at School of Physics and Electronics, Hunan University, Changsha 410082, China.
[i]Also at Guangdong Provincial Key Laboratory of Nuclear Science, Institute of Quantum Matter, South China Normal University, Guangzhou 510006, China.
[j]Also at Frontiers Science Center for Rare Isotopes, Lanzhou University, Lanzhou 730000, People's Republic of China.
[k]Also at Lanzhou Center for Theoretical Physics, Lanzhou University, Lanzhou 730000, People's Republic of China.
[l]Also at the Department of Mathematical Sciences, IBA, Karachi 75270, Pakistan.